Microarray Analysis of the Genome-Wide Response to Iron Deficiency and Iron Reconstitution in the Cyanobacterium *Synechocystis* sp. PCC 6803[1[w]]

Abhay K. Singh, Lauren M. McIntyre, and Louis A. Sherman*

Department of Biological Sciences (A.K.A., L.A.S.) and Computational Genomics and Department of Agronomy (L.M.M.), Purdue University, West Lafayette, Indiana 47907

AQ: A A full-genome microarray of the (oxy)photosynthetic cyanobacterium *Synechocystis* sp. PCC 6803 was used to identify genes that were transcriptionally regulated by growth in iron (Fe)-deficient versus Fe-sufficient media. Transcript accumulation for 3,165 genes in the genome was analyzed using an analysis of variance model that accounted for slide and replicate (random) effects and dye (a fixed) effect in testing for differences in the four time periods. We determined that 85 genes showed statistically significant changes in the level of transcription ($P \leq 0.05/3{,}165 = 0.0000158$) across the four time points examined, whereas 781 genes were characterized as interesting ($P \leq 0.05$ but greater than 0.0000158; 731 of these had a fold change $>1.25\times$). The genes identified included those known previously to be Fe regulated, such as *isiA* that encodes a novel chlorophyll-binding protein responsible for the pigment characteristics of low-Fe (LoFe) cells. ATP synthetase and phycobilisome genes were down-regulated in LoFe, and there were interesting changes in the transcription of genes involved in chlorophyll biosynthesis, in photosystem I and II assembly, and in energy metabolism. Hierarchical clustering demonstrated that photosynthesis genes, as a class, were repressed in LoFe and induced upon the re-addition of Fe. Specific regulatory genes were transcriptionally active in LoFe, including two genes that show homology to plant phytochromes (*cph1* and *cph2*). These observations established the existence of a complex network of regulatory interactions and coordination in response to Fe availability.

Fn1 Fe is an essential element that is required for the growth and development of all organisms, including microorganisms (Hantke, 2001) and plants (Thimm et al., 2001; Negishi et al., 2002). Although Fe is abundant in nature, the availability of this element is very limited because of its poor solubility in aerobic environments. In the presence of oxygen at physiological pH, the rapid oxidation of the ferrous form to the ferric form leads to the precipitation of Fe and its essential unavailability. Thus, living organisms have developed various mechanisms to solubilize Fe to improve its bioavailability (Fox and Guerinot, 1998; Ratledge and Dover, 2000). Fe is of great importance for the growth of both pathogenic and nonpathogenic bacteria, and many strains devote a significant portion of their genome to the regulation of and the acquisition of Fe (Earhart, 1996; Paustian et al., 2001).

Cyanobacteria are (oxy)photosynthetic organisms in which Fe stress has been studied in some detail (Straus, 1994; Behrenfeld and Kolber, 1999). Fe deficiency results in a variety of physiological and morphological changes in cyanobacteria, the most obvious of which is a significant change in cellular pigmentation. The overall changes include: loss of the light-harvesting phycobilisomes (Guikema and Sherman, 1983), changes in the fluorescence and absorption characteristics (Guikema and Sherman, 1983, 1984; Pakrasi et al., 1985a, 1985b), reduction in the number of thylakoids (Sherman and Sherman, 1983), and replacement of proteins with cofactors containing Fe to those with non-Fe cofactors, such as ferredoxin with flavodoxin (Laudenbach and Straus, 1988; Laudenbach et al., 1988; Straus, 1994). Most importantly, a novel chlorophyll (Chl)-binding protein, encoded by *isiA*, is synthesized (Pakrasi et al., 1985b; Laudenbach and Straus, 1988; Burnap et al., 1993). This IsiA protein resembles CP43 (it is sometimes termed CP43′) and has recently been shown to form an 18-mer around the PSI trimer (Bibby et al., 2001; Boekema et al., 2001). This gene is also regulated by salt concentrations (Vinnemeier et al., 1998) and may be the ancestor of the *Prochlorococcus* sp. Chl AQ: B a_2/b_2 light-harvesting protein (Ting et al., 2002). Many other changes are associated with Fe deficiency in cyanobacteria and cells continue to grow, although the growth rate is somewhat lower and the cells are

[1] This work was supported by the National Science Foundation (grant no. MCB–0084457 to Robert Burnap and L.A.S. for the construction of the microarray), by the Department of Energy (grant no. DE–FG92–99ER20342 to L.A.S.), and by the U.S. Department of Agriculture-IFAFS (grant no. NOO14–94-1–0318 to L.M.M.).

AQ: T

[w] The online version of this article contains Web-only data. The supplemental material is available at http://www.plantphysiol.org.

* Corresponding author; e-mail lsherman@bilbo.bio.purdue.edu; fax 765–496–1496.

Article, publication date, and citation information can be found at www.plantphysiol.org/cgi/doi/10.1104/pp.103.024018.

smaller. The addition of Fe to the cultures can reverse these changes, and cells return to normal within 18 to 24 h after the addition of Fe (Sherman and Sherman, 1983; Riethman et al., 1988).

Microarray technology permits an assay of global gene expression patterns under a variety of experimental conditions. These arrays are particularly efficient in organisms for which the entire genome has been sequenced, such as *Synechocystis* sp. PCC 6803, which is now thought to have 3,264 genes (Kaneko et al., 1996; see Cyanobase at http://www.kazusa.or.jp/cyano/cyano.html). Microarrays have been developed for many systems, including for bacteria such as *Escherichia coli* (Richmond et al., 1999; Tao et al., 1999; Arfin et al., 2000) and for plants such as Arabidopsis (Pérez-Amador et al., 2001; Seki et al., 2001). A series of papers have appeared utilizing *Synechocystis* sp. PCC 6803 microarrays (Hihara et al., 2001; Suzuki et al., 2001; Gill et al., 2002; Kanesaki et al., 2002). These arrays have been used to monitor changes in different environmental parameters. The arrays that we constructed, in conjunction with the laboratory of Dr. Rob Burnap (Oklahoma State University, Stillwater), contain (in triplicate) cDNAs up to 2 kb of the 3,165 genes annotated in the Kazusa sequence before May 2002.

The substantial pigmentation changes under Fe-deficient growth provide an easy way to determine the cellular response to Fe deficiency or the redevelopment of the normal phenotype. Thus, Fe deficiency is an ideal system in which to study global gene expression in cyanobacteria. In a previous study, we developed a differential expression using customized amplification library for the analysis of global gene expression in the unicellular cyanobacterium, *Synechocystis* sp. PCC 6803 (Singh and Sherman, 2000). We now extend this study through an analysis of a full-genome microarray of *Synechocystis* sp. PCC 6803. We identified transcriptional changes in many genes that code for proteins involved in assembly or disassembly processes (e.g. chaperones and proteases) and in the structural proteins (e.g. IsiA or phycobiliproteins). The arrays also enabled us to detect genes involved in the regulation of these processes and for those that encode proteins needed for the acquisition and storage of Fe (Katoh et al., 2000, 2001). In this study, we identify many genes that are transcriptionally regulated during Fe deficiency and after the re-addition of Fe and that provide new insights into optimization of biological processes that enable cells to grow during nutrient limitation.

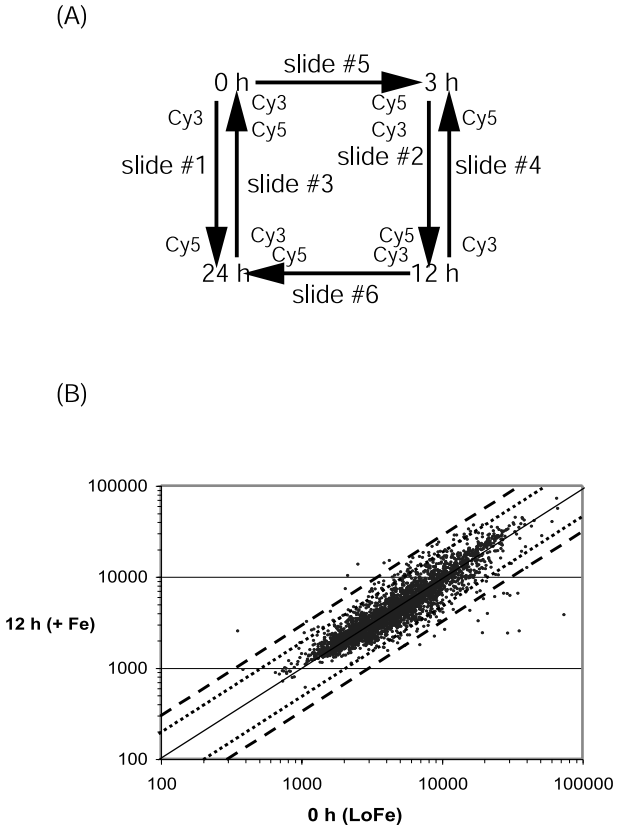

Figure 1. A, Diagrammatic representation of the loop design utilized for identification of differentially expressed genes in response to iron availability. A total of six slides was used with dye swaps between the 0- and 24-h time points and between 3- and 24-h time points. B, Scatter plot that compares the mean spot intensities of 0 h (low iron [LoFe]) and 12 h (+Fe). Data from 0- and 12-h time points were normalized, and their mean signal intensities were plotted. The black line represents equal labeling for the two samples, whereas the dotted (2-fold) and dashed (3-fold) lines identify genes that demonstrated large labeling differences during the hybridization experiment.

RESULTS

Array Data and Statistical Analysis

The loop design utilized in this study is discussed in "Materials and Methods" and outlined in Figure 1A. This approach allows comparison among all conditions via the ANOVA model (Churchill, 2002; Yang and Speed, 2002). We were most interested in determining the changes in gene transcription, as a function of time, between the Fe-deficient and -sufficient states at different time points after the reintroduction of Fe. We previously demonstrated that similar physiological and ultrastructural changes occur as we go from Fe sufficiency to Fe deficiency or vice versa, and these results are inherent in the loop design (Sherman and Sherman, 1983; Riethman et al., 1988). Thus, we compared each of the Fe-sufficient states with the Fe-deficient state to identify the major changes in certain classes of genes that were strongly regulated by the presence/absence of Fe. Therefore, we use the terms induced and repressed to reflect the increase and the decrease, respectively, in the level of transcription from Fe sufficiency to deficiency.

The scatter plot in Figure 1B represents the relationship of the average hybridization intensities of LoFe (0 h) versus 12 h plus Fe. This simple procedure

permitted an overview of the data and indicated that most of the spots fell along the diagonal and were equally labeled. Those spots that fell off the diagonal were candidates for genes with expression changes and lines indicating 2-fold (dotted) and 3-fold (dashed) changes are shown. Some of the published reports on microarray analysis have used an arbitrary cutoff of a 2-fold change to identify differentially expressed genes. However, it has been shown that changes in gene expression smaller than that of 2-fold can be reliably identified (Arfin et al., 2000; Jin et al., 2001; Long et al., 2001; Yue et al., 2001; Oleksiak et al., 2002; Yang et al., 2002). Jin et al. (2001) reported that changes in the gene expression as small as 1.2-fold can be considered as differentially expressed if a robust statistical method is used. We present an ANOVA modeling approach similar to that reported by Oleksiak et al. (2002) that used the same type of experimental design (see "Materials and Methods"). This enabled us to identify genes that displayed differential expression across the four time points examined. We selected genes for additional consideration using a significance level of 0.05 and at least a 1.25-fold change in transcript level intensity.

One advantage of the LoFe system was the known regulation of the *isiAB* genes (up-regulated under Fe-deficient conditions) and the phycobilisome genes (down-regulated under Fe-deficient conditions). We used these genes as markers during the early stages of this study to optimize hybridization conditions and spot analysis. The conditions described in "Materials and Methods" demonstrated a 22-fold increase in *isiA* expression under Fe-deficient conditions with a P value of 6×10^{-10}. The *isiA* gene represented the largest transcriptional increase among all of the genes, whether we analyzed all significant or interesting genes together or by functional category.

Differential Expression in Response to Fe

Using the criteria described in "Materials and Methods," we identified 85 differentially expressed, statistically significant genes and 731 statistically interesting genes. An additional 50 genes that had statistically significant or interesting P values but violated the normality assumption were included in our considerations after careful examination revealed that the heteroscedasticity of variance causing the departure from normality was due to extreme differences between the Fe-deficient and -sufficient states. Table I shows the number of genes differentially T1
expressed in each functional category as defined in
Cyanobase, whereas Table II highlights some specific T2
genes that demonstrated transcriptional changes. The complete statistical analysis for all 3,165 genes can be found in Supplemental Data Table I (see http://www.plantphysiol.org). In addition, the final list of 866 genes examined in the functional analysis can be found in Supplemental Data Table II (see http://www.plantphysiol.org) as can the order of all 866
genes clustered in Figure 3A . The genes that were AQ: E
either up- or down-regulated at different times under Fe-deficient conditions or after the addition of Fe are
plotted in a Venn diagram (Fig. 2). This figure high- F2

Table I. *Differentially regulated genes in response to Fe availability according to functional categories as defined in Cyanobase*

General Pathway	No. of Genes	Differentially Expressed Genes[a]
Amino acid biosynthesis	83	29
Biosynthesis of cofactors, prosthetic groups, and carriers	116	26
Cell envelope	63	13
Cellular processes	61	21
Central intermediary metabolism	31	3
DNA replication, restriction, modification, recom bination, and repair	51	14
Energy metabolism	86	24
Fatty acid, phospholipids, and sterol metabolism	34	5
Hypothetical	449	99
Unknown	1,267	292
Other categories	258	45
Photosynthesis and respiration	129	70
Purines, pyrimidines, nucleosides, and nucleo tides	39	8
Regulatory functions	156	66
Transcription	27	16
Translation	146	81
Transport and binding proteins	169	54
Total	3,165	866

[a] Genes were considered differentially regulated if the fold change was >1.25 and P value was <0.05.

Table II. *A partial list of differentially regulated genes in response to Fe availability based on fold change > 1.25 and P value of the test for the effect of time*

The complete list of the differentially expressed genes identified in this study is in Supplemental Data Table II (http://www.plantphysiol.org). Fold changes: −, decreased transcription in LoFe; positive, increased transcription in LoFe.

Gene	Gene Functional Identification	Fold Change			*P* Value
		0/3	0/12	0/24	
Cellular processes					
Cell division					
Sll1463	Cell division protein FtsH (ftsH)	1.18	1.30	1.48	0.031
slr0228	Cell division protein FtsH (ftsH)	1.34	1.48	1.72	0.0006
slr0374	Cell division cycle protein	1.99	1.46	1.09	0.003
slr1604	Cell division protein FtsH (ftsH)	−1.82	−1.41	−1.99	0.035
Chaperones					
sll0416	60-kD chaperonin 2 (groEL-2)	−2.19	−1.63	1.16	5E-07
sll0430	Heat shock protein (htpG)	1.40	1.43	1.73	0.003
sll1666	DnaJ protein (dnaJ)	1.37	1.46	1.74	0.0002
sll1932	DnaK protein (dnaK)	−1.29	−1.11	−1.49	0.008
slr2075	10-kD chaperonin (groES)	−1.78	−1.51	1.39	0.0001
slr2076	60-kD chaperonin 1 (groEL)	−1.48	−1.82	−1.11	0.033
Energy metabolism					
Glycolysis					
sll0593	Glucokinase (glk)	−1.54	−1.28	−1.08	0.002
sll1196	Phosphofructokinase (pfkA)	−1.11	−1.19	−1.60	0.003
slr0943	Fru-bisphosphate aldolase (fda)	−1.49	−2.31	−3.54	7E-11
slr0952	Fru 16-bisphosphatase (fbp)	1.17	1.63	1.41	0.004
Slr1349	Glc-6-phosphate isomerase (pgi)	−1.09	−1.11	−1.43	0.025
Sugars					
Sll0045	Suc phosphate synthase (sps)	−1.20	−2.50	−3.34	4E-11
Sll1212	GDP-D-Man dehydratase (rfbD)	−1.65	−1.23	−1.03	0.0001
Slr1299	UDP-glucose dehydrogenase	1.00	1.01	−1.47	0.006
Photosynthesis and respiration					
ATP synthase					
Sll1322	ATP synthase subunit a (atpI)	−1.94	−3.19	−2.61	0.0002
Sll1323	ATP synthase subunit b′ (atpG)	−1.11	−1.60	−1.58	0.014
Sll1324	ATP synthase subunit b (atpF)	−2.68	−1.97	−1.28	1E-06
Sll1325	ATP synthase d subunit (atpD)	−1.63	−1.73	−2.31	7E-06
Sll1326	ATP synthase a subunit (atpA)	−1.79	−3.14	−2.16	0.001
Slr1329	ATP synthase b subunit (atpB)	−2.04	−2.01	−1.95	0.0001
Ssl2615	ATP synthase subunit c (atpH)	−2.05	−1.98	−1.95	0.0003
CO_2 fixation					
Sll1028	Carbon dioxide-concentrating mechanism protein (ccmK)	−1.75	−1.88	−2.19	8E-06
Sll1029	Carbon dioxide-concentrating mechanism protein (ccmK)	−1.36	−2.13	−1.95	0.037
Sll1031	Carbon dioxide-concentrating mechanism protein (ccmM)	−1.83	−2.66	−2.10	0.0005
Sll1525	Phosphoribulokinase (prk or ptk)	−1.57	−1.29	−1.24	0.008
Slr0009	Rubisco large subunit (rbcL)	−1.45	−1.59	−1.58	0.002
Slr0012	Rubisco small subunit (rbcS)	−1.69	−1.89	−2.19	1E-06
Cytochrome b_6/f complex					
Slr0343	Cytochrome b6-f complex subunit 4 (petD)	2.65	2.15	2.40	0.00001
smr0003	Cytochrome b6-f complex subunit PetM (petM)	−1.31	−1.49	−1.48	0.002
smr0010	PetG subunit of the cytochrome b6f complex (petG)	−1.38	−2.08	−1.86	0.004
PSI					
sll0629	PSI subunit X (psaK)	1.54	1.05	−1.35	0.031
slr1655	PSI subunit XI (psaL)	−1.26	−1.41	−1.75	0.00004
slr1834	P700 apoprotein subunit Ia (psaA)	−1.37	−1.49	−2.31	0.0002
slr1835	P700 apoprotein subunit Ib (psaB)	−1.11	−1.32	−1.45	0.015
sml0008	PSI subunit IX (psaJ)	−1.07	−1.57	−1.69	0.018
smr0004	PSI subunit VIII (psaI)	−1.30	−1.28	−1.45	0.0002
ssl0563	PSI subunit VII (psaC)	−1.40	−1.63	−2.24	0.0006
ssr2831	PSI subunit IV (psaE)	−1.36	−1.49	−1.73	0.00005
PSII					
sll0247	Fe stress Chl-binding protein (isiA)	10.42	19.29	22.09	6E-10
sll0258	Cytochrome c550 (psbV)	−1.07	−2.13	−2.15	0.002
sll0427	PSII manganese-stabilizing polypeptide (psbO)	−1.49	−2.22	−2.67	0.00002

(*Table continues on following page.*)

Table II. (*Continued from previous page.*)

Gene	Gene Functional Identification	Fold Change			*P* Value
		0/3	0/12	0/24	
sll1194	PSII 12-kD extrinsic protein (psbU)	−1.08	1.03	−1.76	0.0002
slr0906	PSII CP47 protein (psbB)	−1.77	−2.12	−2.42	3E-06
sml0001	PSII PsbI protein (psbI)	−1.24	−1.56	−1.88	3E-06
smr0001	PSII PsbT protein (psbT)	−1.38	−2.36	−2.13	0.004
ssl2598	PSII PsbH protein (psbH)	−1.30	−2.73	−3.37	4E-06
ssr3451	Cytochrome b559 a subunit (psbE)	−1.09	−1.20	−1.28	0.001
Phycobilisomes					
sll1471	Phycobilisome rod-core linker polypeptide (cpcG)	−1.06	−2.65	−2.20	0.0004
sll1577	Phycocyanin b subunit (cpcB)	−1.07	−2.18	−2.68	0.0002
sll1578	Phycocyanin a subunit (cpcA)	−1.93	−2.32	−2.32	1E-06
sll1579	Phycocyanin-associated linker protein (cpcC)	−1.59	−2.50	−3.90	0.00001
sll1580	Phycocyanin-associated linker protein (cpcC)	−1.32	−4.15	−6.19	1E-09
slr0335	Phycobilisome LCM core-membrane linker (apcE)	−1.02	−1.42	−1.87	0.0003
slr1459	Phycobilisome core component (apcF)	−1.16	−1.48	−1.80	3E-06
slr1878	Phycocyanin alpha phycocyanobilin lyase (cpcE)	−1.08	−1.41	−1.50	0.0005
slr1986	Allophycocyanin b chain (apcB)	−1.44	−2.37	−2.11	0.0005
slr2051	Phycobilisome rod-core linker polypeptide (cpcG)	−1.02	−1.38	−1.73	4E-06
slr2067	Allophycocyanin a chain (apcA)	−1.34	−2.51	−3.19	0.00004
ssl3093	Phycocyanin-associated linker protein (cpcD)	−1.47	−2.13	−2.68	1E-07
ssr3383	Phycobilisome LC linker polypeptide (apcC)	−1.44	−1.99	−2.46	0.00001
Soluble electron carriers					
sll0199	Plastocyanin (petE)	1.08	−1.19	−1.38	0.005
sll0248	Flavodoxin (isiB)	14.18	11.59	9.14	8E-11
sll0662	Ferredoxin (bacterial-type ferredoxin family)	2.96	3.83	2.90	0.0002
sll1382	Ferredoxin (petF)	1.34	−1.29	−1.82	0.0001
slr0150	Ferredoxin (petF)	−1.21	−1.88	−2.84	0.00006
slr1643	Ferredoxin-NADP oxidoreductase (petH)	−1.67	−1.23	−1.28	0.018
slr1828	Ferredoxin (petF)	−1.32	−1.99	−2.74	3E-06
ssl0020	Ferredoxin (petF)	−2.13	−1.74	−2.08	0.0004
ssr3184	Ferredoxin	−1.39	−2.03	−2.25	0.0001
Regulatory functions					
sll0821	Putative phytochrome (cph2)	1.52	2.38	2.22	0.00005
sll1408	Regulatory protein PcrR (pcrR)	2.03	1.99	1.78	0.00569
slr0473	Phytochrome (phy or cph1)	1.19	1.34	1.36	0.031
slr0474	CheY subfamily (response regulator, rcp1)	1.49	1.88	1.24	0.036
slr0593	CAMP protein kinase regulatory chain	−1.37	−3.96	−6.18	2E-11
Transcription					
RNA synthesis, modification, and DNA transcription					
sll0184	RNA polymerase sigma factor (sigC)	1.98	2.34	1.76	0.009
sll0306	RNA polymerase sigma factor (sigB)	1.49	1.77	1.62	0.011
sll0856	RNA polymerase sigma-E factor (sigH)	−1.09	1.08	1.43	0.00008
sll1689	RNA polymerase sigma factor (sigE)	−1.43	−1.45	−1.04	0.003
sll1787	RNA polymerase beta subunit (rpoB)	1.02	1.03	1.85	6E-06
sll1818	RNA polymerase alpha subunit (rpoA)	−1.36	−1.18	1.49	0.004
sll2012	RNA polymerase sigma factor (sigD)	1.74	2.07	2.41	7E-06
slr0083	ATP-dependent RNA helicase DeaD (deaD)	−1.13	1.54	2.06	0.0005
slr0653	RNA polymerase sigma factor (sigA)	1.72	2.19	2.27	0.0004
slr1545	RNA polymerase sigma-E factor (sigG)	1.02	−1.01	−1.52	0.0004
Translation					
Degradation of proteins, peptides, and glycopeptides					
sll0020	ATP-dependent Clp protease regulatory subunit (clpC)	2.49	3.23	2.28	0.0002
sll0535	ATP-dependent protease ATPase subunit (clpX)	1.16	1.50	1.89	0.001
slr0008	Carboxyl-terminal processing protease (ctpA)	−1.79	−1.75	−1.75	0.006
slr0156	ClpB protein (clpB)	−1.47	−1.47	−1.05	0.0009
slr0164	ATP-dependent Clp protease proteolytic subunit (clpP)	1.33	1.68	1.77	0.0009
slr0165	ATP-dependent Clp protease proteolytic subunit (clpP)	1.65	2.16	2.3	5E-06
slr1204	Serine protease HtrA (htrA)	1.15	1.52	1.64	0.09532

(*Table continues on following page*)

Table II. (*Continued from previous page*)

Gene	Gene Functional Identification	Fold Change			*P* Value
		0/3	0/12	0/24	
Protein modification and translation factors					
sll1110	Peptide chain release factor (prfAor sueB)	−1.25	1.03	1.48	0.007
sll1980	Thioldisulfide interchange protein (trxA)	1.11	1.15	1.47	0.041
slr0974	Initiation factor IF-3 (infC)	−1.56	−1.36	1.43	0.0002
slr1251	Peptidyl-prolyl cis-trans isomerase (cypor rot1)	−1.71	−1.24	1.12	0.00003
slr1549	Polypeptide deformylase (defor fms)	1.44	2.20	2.20	0.007
Transport and binding proteins					
sll0374	High-affinity branched-chain amino acid transport protein	1.20	1.01	1.40	0.04024
sll0385	ABC transporter	1.19	1.18	1.57	0.00076
sll0738	Molybdate-binding periplasmic protein (modA)	−1.30	1.10	−1.10	0.00535
sll0739	ABC transporter	−1.39	−1.22	−1.39	0.00779
sll1404	Biopolymer transport ExbB protein (exbB)	1.65	1.05	1.44	0.05697
sll1405	Biopolymer transport ExbD protein homolog	2.54	1.92	1.43	0.01111
sll1406	Ferrichrome-Fe receptor (fhuA)	2.11	2.08	2.30	9.6E-07
sll1409	Ferrichrome-Fe receptor (fhuA)	1.09	−2.06	−2.77	7.3E-08
sll1878	ABC transporter	2.34	2.35	2.29	1.4E-07
slr0074	ABC transporter subunit (ycf24)	−1.23	−1.52	−1.66	7.4E-08
slr0513	Periplasmic Fe-binding protein	3.79	4.25	3.80	2.9E-07
slr1200	High-affinity branched-chain aa transport protein (livH)	2.23	2.30	2.54	4E-06

lights the transcriptional changes in this system. It is notable that two-thirds of the genes that display differential expression were down-regulated in the Fe-deficient state and that nearly one-third (183/601) had decreased transcription in the Fe-deficient state compared with all three Fe-sufficient states.

We used hierarchical clustering to explore the differential expression as a function of time after the addition of Fe (Fig. 3, A and B). Six of the kinetic categories are diagrammed in Figure 3C and are numbered based on their position from top to bottom within Figure 3A. Category 1 represented the largest group ($n = 437$) and included approximately 50% of these differentially expressed genes. The genes in this category included those involved in photosynthesis, the biosynthesis of pigments, energy metabolism, regulatory functions, translation, and transport. Interestingly, 190 genes within this category have not yet been assigned a specific function. The expression pattern of photosynthetic genes after the addition of Fe, present in category 1, is further represented in Figure 3B and demonstrated that photosynthesis genes were transcriptionally regulated by Fe (repressed in Fe deficiency and induced upon re-addition of Fe). The second category ($n = 74$) included genes involved in translational processes, especially genes coding for ribosomal proteins. Category 3 ($n = 42$) also included some of genes coding for ribosomal proteins and genes involved in transport process. Transcription of genes in categories 2 and 3 increased soon after Fe addition and then reached a plateau or decreased. Categories 4 and 5 demonstrated rather complex kinetics and consisted of many unknown genes. About 80% of the genes in category 4 ($n = 26$) were those assigned only hypothetical structures or functions at present. A majority of genes in category 5 (46/79) had no known function, although the category also included a few genes involved in regulatory functions or in photosynthesis. Category 6 ($n = 202$) included those genes (e.g. *isiA*, *isiB*, *idiA*, transport proteins, proteases, and regulatory proteins, such as sigma factors) whose transcript levels decreased rapidly after the addition of Fe.

Energy Metabolism

We were most interested in identifying differentially transcribed genes by functional category, and we will present data that are pertinent to fundamental cellular processes in cyanobacteria and plants. A relatively small number of genes involved with basic energy metabolism or central intermediary metabolism demonstrated significant changes, and the net effect of this regulation was to lower the breakdown of Glc and promote the storage of carbohydrates in the form of glycogen. A key feature was the down-regulation in Fe-deficient conditions of three genes in the heart of the glycolysis pathway: phosphofructokinase (*pfkA*; sll1196; $P = 0.003$), Glc-6-phosphate isomerase (*pgi*; slr1349; $P = 0.025$), and Fru-bisphosphate aldolase (*fda*; slr0943; $P = 7 \times 10^{-7}$). In addition, Suc phosphate synthetase (*sps*; sll0045; $P = 4 \times 10^{-11}$) transcription was strongly depressed in Fe-deficient conditions, and this may also help route sugars toward glycogen accumulation in these cells (Sherman and Sherman, 1983). Transcription for UDP-Glc dehydrogenase (slr1299; $P = 0.006$) also decreased, but there were only minor changes in the *glgA* and *glgC* genes (encoding proteins involved in glycogen synthesis). There was also enhanced tran-

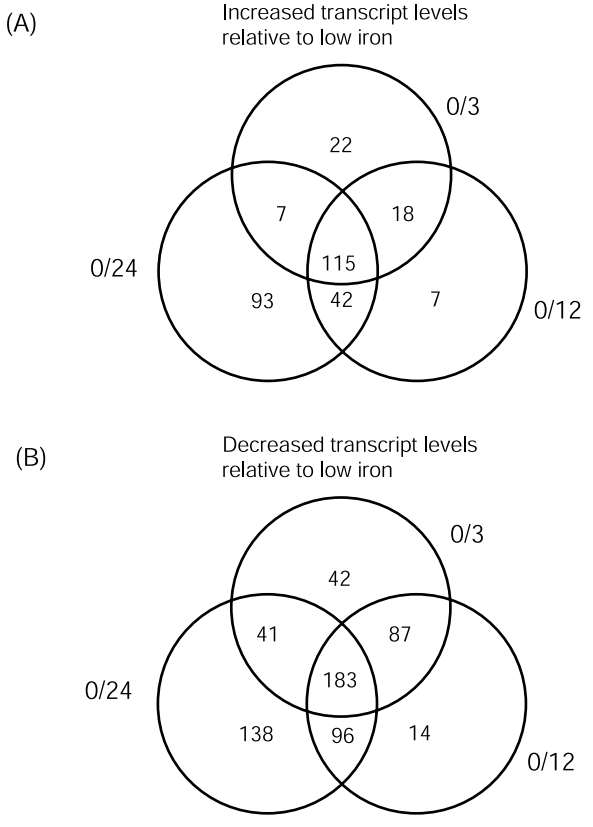

Figure 2. Venn diagrams that display the number of iron-responsive, differentially expressed genes. Three sample pairs (0/3, 0/12, and 0/24) were compared for increased (A) and decreased (B) transcript levels in response to iron availability. All of the genes had a fold change > 1.25 and $P < 0.05$. The numbers in the overlapping areas indicate genes that exhibited differential expression in either two or three sample pairs. The numbers in the nonoverlapping areas indicate the number of genes that exhibited differential expression in one sample pair.

scription of 6-phosphogluconate dehydrogenase (*gnd*; sll0329), and this should lead to enhanced activity of the oxidative branch of the pentose phosphate pathway.

The isiAB Region

The induction of the *isiA* gene is the signature change in cyanobacteria grown in Fe-deficient conditions, and *isiA* had the largest fold change (22-fold) and a *P* value of 6×10^{-10}. We identified a set of five genes starting from sll0247 that showed enhanced transcription in the Fe-deficient state relative to Fe-sufficient conditions (Fig. 4). The fold changes for all of the genes in this cluster were substantial, and the *P* values were all less than 4×10^{-5}. These genes code for proteins of many different functions, including a Chl protein (sll0247; 22-fold, $P = 6 \times 10^{-10}$), a flavodoxin (sll0248; 14-fold, $P = 8 \times 10^{-11}$), a putative pantothenate metabolism flavoprotein (sll0250; 2.4-fold, $P = 4 \times 10^{-5}$), and two genes with no functional designation (sll0249; 14-fold, $P = 9 \times 10^{-10}$; and ssl0461; 2.2-fold, $P = 0.004$). Analysis of several cyanobacterial genomes showed that *isiA* is not contiguous to *isiB* in all cases, whereas the other four genes are found in two clusters (the homologs of sll0248 and sll0249 are contiguous, as are the homologs of ssl0461 and sll0250; data not shown).

Pigment Biosynthesis

One of the more striking transcriptional patterns involved the Chl biosynthetic pathway (Table III). None of the genes in the first one-third of the pathway (*gltX* to *hemE*) demonstrated statistically significant or interesting changes in transcription. However, the genes coding for six of the next seven enzymatic reactions along the main pathway were down-regulated approximately 1.4- to 6.3-fold in Fe-deficient conditions relative to Fe sufficiency (Table III). Protoporphyrin IX is the common branch point for the synthesis of Chl and heme and is converted to heme by ferrochelatase (plus Fe). Interestingly, transcription of the ferrochelatase gene (*hemH*, slr0839; $P = 0.08$) changed very little in response to changes in Fe levels. Finally, the genes coding for the last two enzymes in the pathway were up-regulated in Fe-deficient conditions: protochlorophyllide oxidoreductase (*pcr*; slr0506 $P = 0.014$) and Chl synthetase (*chlG*; slr0056 $P = 0.01$). In addition, a putative gene involved in bilin synthesis, heme oxygenase (*ho1*, sll1184 $P = 0.02$) was down-regulated in Fe-deficient conditions.

Photosynthesis Genes

The photosynthesis genes represent a complicated series of adaptations to the Fe-deficient state (Table II; Fig. 3, A and B). Many of the genes encoding the PSII structural proteins were transcribed at high levels under all conditions and were not transcriptionally regulated by Fe; e.g. *psbA2*, *psbA3*, both *psbD* genes, and *psbC*. The most significant transcriptional change in PSII was the decline in *psbB* of approximately 2.4-fold under Fe-deficient conditions ($P = 3 \times 10^{-6}$). Similarly, all three lumenal proteins that are involved with the regulation of O_2 evolution (*psbO*, *psbU*, and *psbV*) decreased approximately 2-fold in LoFe (*P* values $= 2 \times 10^{-5}$, 2×10^{-4}, and 2×10^{-3}, respectively). This fact may be of great importance for the assembly/disassembly of PSII. Transcription of *psbH* and *psbI* declined rather significantly under Fe-deficient conditions, with *psbH* some 3-fold lower relative to Fe-sufficient cells ($P = 4 \times 10^{-6}$) and *psbI* some 2-fold lower ($P = 3 \times 10^{-6}$). PSI demonstrated a somewhat different type of adaptation, and all statistically interesting genes had lower transcript levels in LoFe (Table II). The reaction center genes (*psaAB*) were transcribed at quite high levels in the Fe-deficient state but rose to even higher levels (1.6–2.0-fold increases; $P = 2 \times 10^{-4}$ and 0.015,

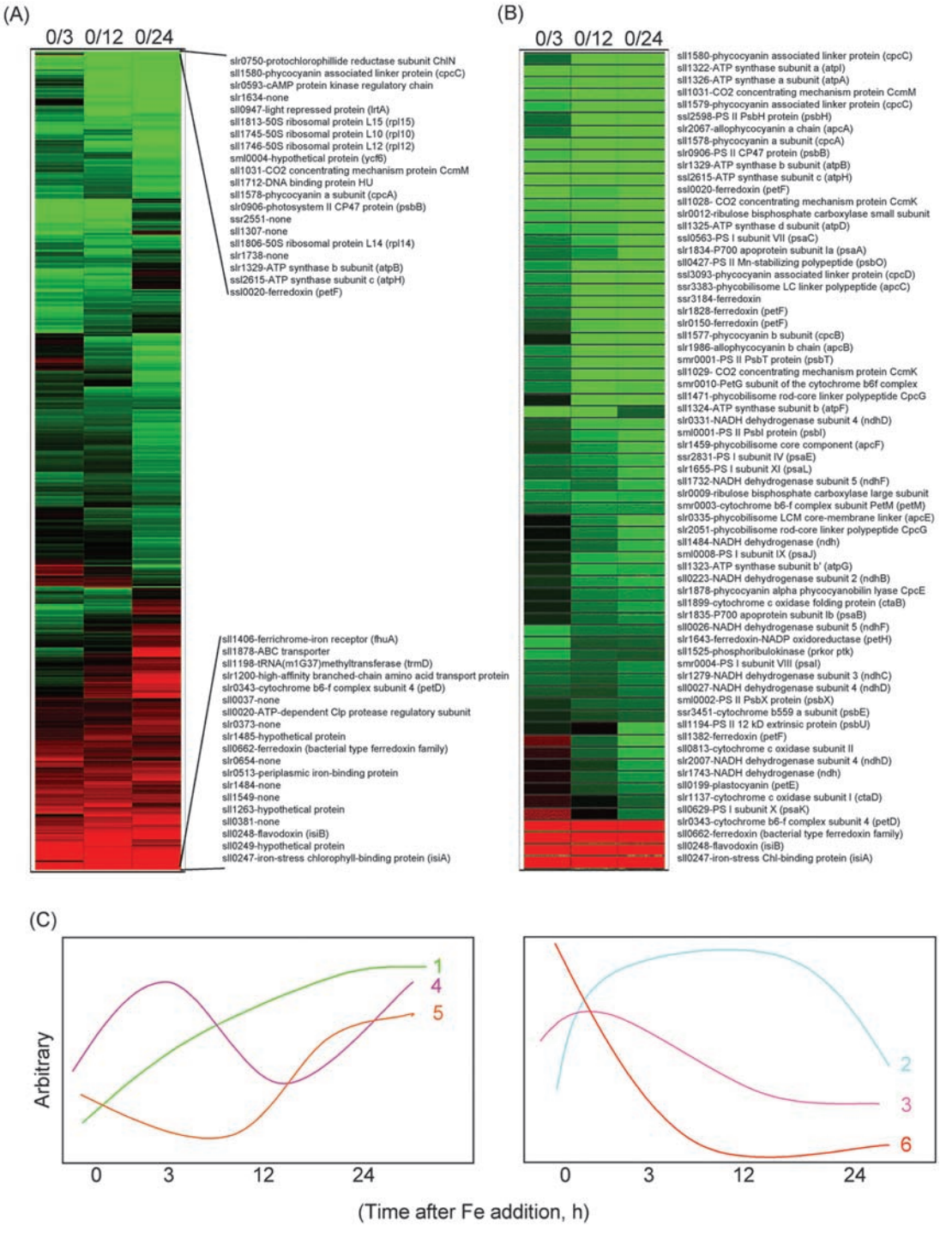

COLOR

AQ: U

Figure 3. A, Hierarchical cluster display of 866 genes that were used for the functional analysis of the iron-responsive differential expression changes. The expression ratio was calculated relative to time point 0 h (i.e. 0/3, 0/12, and 0/24) and were converted to log scale. These values were then used to cluster genes using Spotfire Decisionsite version 7.0 (XXXX, XXXX, XX). Euclidean distance was used as measure of similarity between profiles. The various profiles were clustered by using the weighted pair group method with arithmetic mean. The identification of all genes in this diagram is provided in Supplemental Data Table III (http://www.plantphysiol.org). B, Hierarchical cluster display of genes involved in photosynthetic processes that exhibited fold change of >1.25 and *P* value of <0.05. C, Schematic representation of various patterns of differentially expressed genes in response to iron availability. The various patterns were generated based on the clustering of genes (860/866) in A and numbered accordingly from top to bottom. The *x* axis represents the time-dependent expression of genes after the addition of Fe, whereas the *y* axis represents the transcript level on an arbitrary scale. The number of genes in each category is: 1 (n = 437), 2 (n = 74), 3 (n = 42), 4 (n = 26), 5 (n = 79), and 6 (n = 202).

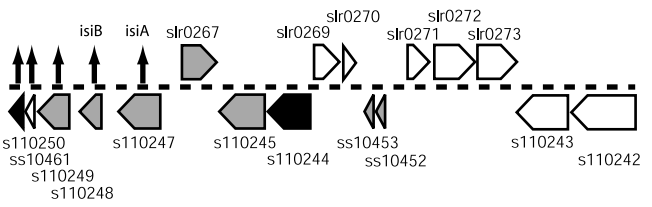

Figure 4. The *isiA* region of the genome in which gene expression was enhanced in LoFe cells. The arrows indicate those five genes that demonstrated an increase in transcription in LoFe cells, and the size of the boxes corresponds to the lengths of the open reading frames.

respectively) during normal growth. Subunits that demonstrated some downward Fe regulation in the Fe-deficient state were *psaC* (2.2-fold, $P = 6 \times 10^{-4}$), *psaE* (1.7-fold, $P = 5 \times 10^{-5}$), *psaI* (1.5-fold, $P = 2 \times 10^{-4}$), *psaJ* (1.7-fold, $P = 0.018$), *psaK* (1.4-fold, $P = 0.013$), and *psaL* (1.8-fold, $P = 4 \times 10^{-5}$). The *psaC* subunit includes a [4Fe-4S] Fe-sulfur cluster, so this 2-fold drop in transcription was understandable. Other photosynthesis complexes were also affected by Fe deficiency. The main ATPase operon, sll1322-sll1328, was down-regulated about 2-fold under Fe-deficient conditions (Table II), although statistically significant or interesting results were not obtained for the operon encoding the β- and ϵ-subunits. The regulation of the cytochrome (cyt) b_6/f complex was both simple and surprising. The *petD* gene was up-regulated some 2.5-fold in the Fe-deficient state ($P = 1 \times 10^{-5}$), whereas the transcription of the other genes encoding the cyt b_6, cyt f, and Rieske Fe-S proteins did not change appreciably. The *petG* and *petM* genes, on the other hand, were down-regulated some 1.6- to 2.0-fold in Fe deficiency. Many of the genes encoding subunits of the NADH dehydrogenase complex were transcriptionally down-regulated, whereas three of the genes encoding components of the cyt c oxidase underwent a series of changes (data not shown). Transcription of these genes was high in the Fe-deficient state, decreased soon after the addition of Fe, but then surpassed the levels of gene expression in the Fe-deficient state 24 h after Fe addition.

The cell employed different regulatory strategies for the soluble proteins or complexes (Table II; Fig. 3B). The soluble carriers responded as expected—the flavodoxin (*isiB*) gene was strongly induced in Fe-deficient conditions, whereas most ferredoxins were down-regulated in the Fe-deficient state. An exception was sll0662 ($P = 2 \times 10^{-4}$), annotated as a bacterial-type ferredoxin, for which the transcript levels increased 3- to 4-fold in the Fe-deficient state compared with the Fe-sufficient states. The phycobilisome genes acted in concert, and virtually all of them were repressed in the Fe-deficient states (Table II). All 12 of the genes encoding phycobilisome complex proteins were statistically significant or interesting and were down-regulated 1.5- to 3.0-fold, as expected from previous spectral data (Guikema and Sherman, 1983, 1984). Among the CO_2 fixation genes, the *rbcLS* genes were down-regulated 1.6- to 2.2-fold ($P = 1 \times 10^{-6}$ and 1.6×10^{-3}, respectively), as were the genes encoding proteins involved in the CO_2-concentrating mechanism.

Transport Proteins

The interactions and complexities among cellular systems were never more apparent than within the transport proteins. As shown in Table I, a large number of transport genes were regulated in the Fe-deficient state, including many ABC transporters. The microarray data show that the following specific genes that encode putative transport proteins are up-regulated in the Fe-deficient state: Leu/Ile/Val uptake (*livFH*; sll0374 and slr1200), cobalt uptake (*cbiMO*; sll0383 and sll0385), and molybdate uptake (sll0738 and sll0739; Table II; see Supplemental Data Table II at http://www.plantphysiol.org). One putative Fe transport gene that demonstrated Fe regulation was *futC* (sll1878; 2.3-fold increase, $P = 1 \times 10^{-7}$). Transcription for the ferrichrome-Fe receptor gene *fhuA* (sll1409; $P = 7 \times 10^{-8}$) dropped sharply in the Fe-deficient state, whereas the periplasmic Fe-binding protein slr0513 increased more than 4-fold ($P = 3 \times 10^{-7}$) in the Fe-deficient state. Interestingly, transcription of the slr0074 gene, an ABC transporter subunit that is related to chloroplast ycf24, also dropped significantly ($P = 7 \times 10^{-8}$) in Fe deficiency.

Transcription and Translation

We observed transcriptional changes in all five Group 1 and Group 2 sigma factors, described in Cyanobase: Group 1, the primary σ-factor, slr0653 (2.3-fold, $P = 0.0004$); and Group 2, the nonessential σ-factors, sll2012 (2.4-fold, $P = 7 \times 10^{-6}$); sll0184 (2.3-fold, $P = 0.009$); sll0306 (1.8-fold, $P = 0.01$); and sll1689 (−1.4-fold, $P = 0.003$). Changes in *rpoAB* transcript accumulation were also found (sll1184, $P = 0.004$; sll1787, $P = 6 \times 10^{-6}$, respectively), but the magnitude of the changes was more modest (Table II).

One of the most obvious features of cells grown in the Fe-deficient state is the drop in protein synthesis and cell-doubling time (Guikema and Sherman, 1983, 1984). The corresponding effect on the transcription of the ribosomal proteins was clearly demonstrated in the microarray experiment. Forty-seven of the genes encoding ribosomal proteins had a drop in transcript levels in the Fe-deficient state of approximately 2-fold that were considered to be statistically significant or interesting (see Supplemental Table II at http://www.plantphysiol.org). This included most of the genes in the major cluster of ribosomal protein genes (sll1799, $P = 4 \times 10^{-5}$ to sll1822, $P = 0.01$). We also noted that the transcript levels of proteins involved in various translation modification

Table III. *Effect of LoFe growth on transcription of genes in the pigment synthesis pathway*

Enzyme	Gene Name	Gene Designation	Regulation in LoFe (+, ↑; −, ↓)	*P* Value
Chl Biosynthesis				–
Glu-tRNA synthetase	*gltx*	s110179	–	–
Glu-tRNA reductase	*hemA*	slr1808	–	–
Glutamate-1-semialdehyde aminotransferase	*hemL/gsa*	s110117	–	–
PBG synthase	*hemB*	s111994	–	–
Porphobilinogen deaminase	*hemC*	slrl887	–	–
Uroporphyrinogen III synthase	*HemD*	s110166	–	–
Uroporphyrinogen III decarboxylase	*hemE*	s1r0536	–	–
Coproporphyrinogen III oxidase	*hemF*	s111185	−1.6× (12 h)	0.0015
	$O_{2\ indep.}$	s111876	−4.0× (12 h)	2×10^{-8}
	hemN	s1l1917	−1.5× (12 h)	0.0026
Protoporphyrinogen IX oxidase	*hemK*	s111237	–	–
Ferrochelatase	*hemH*	slr0839	–	–
Magnesium chelatase	*ch11*	slr1030	–	–
	ChlH	slr1055	–	–
	ChlD	slr1777	−1.8×	5×10^{-5}
Mg-protoporphyrin IX methyl-transferase	*ChlM*	slr0525	−1.5×	0.02
Cyclase	*BchE*	slr0905	−3.4×	2×10^{-8}
Protochlorophyllide reductase	*chlN*	slr0750	−6.3× (12 h)	6×10^{-8}
	chlB	slr0772	–	–
Light induced, Fe subunit	*chlL*	slr0749	–	–
	bchB (or bchK)	ssr2049	−1.4×	0.04
Protochlorophyllide oxidoreductase	*pcr*	slr0506	+1.5×	0.014
Chl synthetase	*chlG*	slr0056	+1.7×	0.01
Phycobilin synthesis				
Heme oxygenase	*ho1*	sllll84	−1.6×	0.02
	ho2	slll875	–	–
Biliverdin reductase	*bvdR*	slr1784	–	–

events were also affected by Fe levels (Table II). For example, transcript levels of peptidyl-prolyl cis-trans-isomerase declined significantly in LoFe cells (slr1251, 1.7-fold, $P = 3 \times 10^{-5}$), whereas polypeptide deformylase increased steeply (slr1549, 2.2-fold, $P = 0.007$).

Other Regulatory Genes

A number of regulatory genes were differentially expressed during growth in different Fe concentrations. The largest change was in slr0593 (−6.25-fold, $P = 2 \times 10^{-11}$), the putative cAMP protein kinase regulatory chain. This gene was repressed in the Fe-deficient state and accumulated to high transcript levels after Fe addition. Genes encoding phytochromes represent another important regulatory class that was strongly up-regulated in the Fe-deficient state. These genes included the two-component regulatory system slr0473/slr0474 in which slr0473 (1.4-fold, $P = 0.03$) is the phytochrome-like gene *cph1*, and slr0474 (1.9-fold, $P = 0.04$) is the response regulator *rcp*1 (closely related to *cheY*; Yeh et al., 1997; Garcia-Dominguez et al., 2000; Park et al., 2000b; Lamparter et al., 2001). A second putative phytochrome (termed *cph2*; sll0821; 2.4-fold, $P = 5 \times 10^{-5}$) has been identified (Park et al., 2000a; Wilde et al., 2002), and this gene was also strongly up-regulated under Fe-deficient conditions (Table II).

AQ: F

Cellular Processes. Cell Division, Chaperones, and Proteases

The transcription of many of the genes involved in basic cellular processes, such as chaperones and proteases, was increased by 2- to 3-fold under Fe-deficient conditions relative to 24 h, and it often decreased rapidly after Fe addition. The proteases that were altered in the Fe-deficient state included three *ftsH* genes: slll463 (1.5-fold, $P = 0.03$), slr0228 (1.7-fold, $P = 0.0006$), and slr1604 (0.5-fold, $P = 0.04$). Other LoFe-induced proteases included subunits of the ClpP complex: *clp*C (sll0020, 3.2-fold, $P = 0.0002$), *clpP3* (slr0165, 2.3-fold, $P = 5 \times 10^{-6}$), *clpP4*,(slr0164, 1.8-fold, $P = 0.0009$), and *clpX* (sll0535, 1.9-fold, $P = 0.001$). Importantly, slr0008 (−1.7-fold, $P = 0.006$), the carboxyl-terminal-processing protease (*ctpA*), decreased significantly in LoFe, consistent with the decrease in PSII assembly.

Chaperones also demonstrated interesting transcriptional changes, including *htpG* (hsp90, sll0430, 1.7-fold, $P = 0.003$), *dnaJ* (slll666, 1.7-fold, $P = 0.0002$), *dnaK* (sll1932, − 1.4-fold, $P = 0.008$), *groELS* (slr2075, − 1.7-fold, $P = 1 \times 10^{-4}$; and slr2076, − 1.7-fold, $P = 0.03$), and *groEL-2* (sll0416, − 2.0-fold, $P = 5 \times 10^{-7}$). In the case of the GroELS proteins, the transcript accumulation increased strongly immediately after the addition of Fe and then settled down to a steady-state level that was lower than under Fe-

deficient conditions. Another protein with chaperone activity is slr0374 (2.0-fold, $P = 0.003$), a protein previously identified as Fe induced (Singh and Sherman, 2000). We have subsequently determined that the gene is part of an operon with slr0373 (3.0-fold, $P = 8 \times 10^{-6}$), slr0374, and slr0376 (2.6-fold, $P = 7 \times 10^{-6}$) and that the operon is induced under many stress conditions (Singh and Sherman, 2002).

DISCUSSION

In this study, we utilized DNA microarray technology to profile the genes that were differentially expressed during growth of *Synechocystis* sp. PCC 6803 in Fe-deficient versus Fe-reconstituted medium. The results paint a rather detailed picture of how this cyanobacterium responds to growth in Fe-deficient versus Fe-reconstituted medium. Transcription of the protein synthesis machinery was decreased substantially, transcription of genes encoding proteins involved in protein modification, assembly, or degradation was altered, and glycolysis genes were turned down in the Fe-deficient state. These changes resulted in a cell that was smaller, had fewer photosynthetic membranes, and utilized less energy. Glc utilization was slowed and glycogen synthesis enhanced—this leads to the accumulation of glycogen granules as was documented by electron microscopy (Sherman and Sherman, 1983). The results indicated that the cell responds immediately to the presence of Fe by synthesizing proteins needed for energy production and pigment biosynthesis. It then devotes a significant period to the assembly of the translational machinery, and these genes are eventually turned off. Those genes involved with cell maintenance under Fe-deficient conditions are efficiently repressed upon the presence of Fe.

When cells are grown under Fe-deficient conditions, a variety of physiological and morphological phenomena occur, the most obvious of which is a significant change in cellular pigmentation and the reorganization of photosynthetic complexes (Guikema and Sherman, 1983, 1984; Pakrasi et al., 1985a, 1985b; Laudenbach and Straus, 1988; Laudenbach et al., 1988; Straus, 1994). Data presented here showed that the major PSII genes were not the targets of transcriptional control. The transcription of the PSII reaction center genes remained high in the Fe-deficient state and changed little after the addition of Fe. Instead, significant changes occurred in genes, which suggested that posttranscriptional regulation played a significant role under these conditions. For example, *psbB*, *psbH*, *psbI*, and those coding for oxygen-evolving proteins that are located in the thylakoid lumen (*psbO*, *psbU*, and *psbV*) were down-regulated in the Fe-deficient state. It has been shown recently that a *Synechocystis* sp. PCC 6803 *psbH* mutant, which resulted in the absence of PsbH, destabilized PSII (Komenda et al., 2002). In addition, the 3.8-Å crystal structure of PSII indicates that both PsbH and PsbI are localized near the interface of the D2 and CP47 (PsbB) proteins (Zouni et al., 2001; Heathcote et al., 2002). Thus, the lowering of the transcript levels of *psbB*, *psbH*, and *psbI* is consistent with a tendency to disassemble or to destabilize PSII. These changes were also coordinated by the regulation of two key enzymes involved in PSII assembly processes. The growth of *Synechocystis* sp. PCC 6803 in the Fe-deficient conditions resulted in transcriptional increases for the *ftsH* (slr0228) gene. This gene has been suggested to be involved in D1 protein degradation in cyanobacteria and in Arabidopsis (Lindahl et al., 2000; Mann et al., 2000; Hauβühl et al., 2001; Bailey et al., 2002). Similarly, transcription of the gene encoding *ctpA*, the carboxy-terminal protease involved in D1 protein processing, was reduced significantly in response to LoFe. These results were consistent with the cellular tendency to enhance PSII instability.

A similar regulation was also observed for PSI ,and the genes that were regulated by Fe tend to destabilize PSI. For example, down-regulation under Fe-deficient conditions of PsaE, a stromal protein, and PsaK, an intrinsic PSI component, was important because these proteins are required for the stable assembly of PSI (Xu et al., 2001). Similarly, PsaI (important for the normal organization of the PsaL subunit that is required for PSI trimer formation in cyanobacteria) was also down-regulated (Fromme et al., 2001; Xu et al., 2001). In addition, the PSI *psaAB* reaction center genes were down-regulated some 2-fold under Fe-deficient conditions. All of these changes are aimed at destabilizing the PSI complex or at ensuring that fewer functional PSI complexes can be assembled, especially in their trimeric form. Thus, the cell was attempting to balance the stoichiometry among the different complexes; the net result is a PSI:PSII ratio that is much closer to 1:1 than the 3:1 found in cells grown under Fe sufficiency (Riethman et al., 1988).

When cells were transferred to Fe-deficient conditions, Chl and phycobilin content declined and remained at a basal level sufficient for a limited photosynthetic apparatus. Genes encoding phycobilisome proteins were reduced to an appropriate lower level commensurate with the presence of a lower level of phycobilin pigments. However, transcript levels of genes encoding proteins involved in pigment biosynthesis showed interesting differences. Intermediates needed for heme biosynthesis were maintained, whereas intermediates after protoporphyrin IX were decreased. However, any of the later intermediates can be rapidly converted into Chl due to an increase in enzyme availability of the oxidoreductase and the Chl synthetase. This pattern may suggest a fine-tuning of the metabolic intermediates to ensure that Chl levels are commensurate with the Chl-binding proteins that are synthesized.

Genes encoding phytochromes represent an important regulatory class that was strongly up-regulated in the Fe-deficient state. Both *cph1* and *cph2* were also dark induced and light repressed (Park et al., 2000a). Although it has been postulated that Cph1 (and also Cph2) are involved in the regulation of events during the light/dark or dark/light transitions, no strong phenotype was obtained with a *cph1* knockout mutant (Garcia-Dominguez et al., 2000). However, a clue to function came from an experiment in which a *cph2* mutant and a *cph1/cph2* double mutant responded differently than wild type and moved toward a blue light source. One interpretation of this result was that Cph2 is needed for an inhibition of positive mobility toward blue light. Our results suggested that the putative phytochromes might have a function during the cellular response to Fe stress. We will analyze mutants in these genes to determine how the mutants grow and respond under LoFe conditions.

A large number of transport genes, including many ABC transporters, were regulated by Fe. Such results were in agreement with the idea that Fe-deficient cells do everything possible to bring ions and other metabolites into the cell to develop a modified metabolic state and that the Fe inducibility of various transport genes resulted from a strong cellular response to nutrient limitation. A particular interesting Fe-regulated protein is IdiA (Michel et al., 1996, 1999, 2001). The protein (now ascribed to slr1295 and not slr0513) is thought to have a protective role for the acceptor side of PSII during Fe stress, and it has been shown to be located at the thylakoid lumen in *Synechocystis* sp. PCC 6803 (Tölle et al., 2002). Quite interestingly, we found that slr1295 was not significantly Fe regulated ($P = 0.167$), whereas slr0513 was one of the genes with the largest, and most significant, fold increase (approximately 4.5-fold, $P = 3 \times 10^{-7}$) between the Fe-deficient state and 24 h after Fe addition. The transcription of slr1295 also was shown to be cold repressible by some 3-fold (Suzuki et al., 2001) and light inducible (Gill et al., 2002). Thus, this protein may be most important for oxidative protection in *Synechocystis* sp. PCC 6803 due to environmental factors in addition to Fe starvation.

A plethora of genes that currently have no known functional designation were regulated by Fe availability. Such findings provide the impetus for future microarray experiments with cells grown under different environmental conditions and with the many knockout mutants that we can produce. A first start at functional analysis of these genes has come from cluster analysis of the genes that were up- or down-regulated under specific conditions. For example, slr0374 was identified as a Fe-responsive gene in our previous work (Singh and Sherman, 2000); then, we determined that slr0374 and the neighboring genes (slr0373, slr0374, and slr0376) represented an operon (Singh and Sherman, 2002). All three genes are strongly transcribed under LoFe conditions compared with Fe-sufficient conditions and appeared to be involved in the periplasm in some type of chaperone activity of membrane protein assembly (A.K. Singh and L.A. Sherman, unpublished data). Thus, the microarray data identified genes that represent the focus of more intensive research with genetics and physiology to determine gene function, their chromosomal organization, and their mode of regulation. We will continue such efforts, with an emphasis on the assembly/disassembly of the photosynthetic complexes and especially on the interaction of the novel IsiA protein with both PSII and PSI.

MATERIALS AND METHODS

Strain and Growth Conditions

Glassware used in LoFe medium preparation was treated with EDTA, and the LoFe BG-11 medium was made as follows. Ferric ammonium citrate present in normal BG-11 medium was replaced with ammonium citrate for the LoFe medium, and four of the BG-11 stock solutions ($NaNO_3$, ammonium citrate, K_2HPO_4, and Na_2CO_3) were passed through Chelex-100 (Bio-Rad Laboratories, Hercules, CA) columns to eliminate trace amounts of Fe. *Synechocystis* sp. strain PCC 6803 cells were subcultured in LoFe media at least 6 d before experimental use. Cells were grown phototrophically in LoFe medium at 30°C under a light intensity of 20 to 30 μE m^{-2} s^{-1}. The culture was bubbled vigorously by air. Recovery of Fe-deficient cultures was accomplished by addition of 6 mg of ferric ammonium citrate per liter of medium, a concentration equal to that present in the normal BG-11 medium. Cells were removed during recovery at 0 h (iron-deficient culture) or at 3, 12, and 24 h after the addition of iron (reconstituting cultures) and harvested by centrifugation at 4,000*g* in a refrigerated centrifuge. Cells were either frozen and stored at −80°C or immediately used for RNA isolation.

Construction of DNA Array

The complete description of array construction will be described elsewhere (B. Postier, A. Singh, L.A. Sherman, and R.B. Burnap, unpublished data). In brief, we utilized a two-stage PCR process to amplify 3,165 genes identified on the *Synechocystis* sp. PCC 6803 genome on the Kazusa Web site before May 2002. The first stage of PCR was based on a bipartite primer that contained both gene-specific and universal sequences to amplify the individual genes using genomic DNA as template. The gene-specific sequences were of variable length to allow uniform annealing temperatures, and longer genes (230 of 3,165) were truncated at the 3′ end to 2 kb. The second stage PCR involved the amplification of first stage products with primer corresponding to the universal sequence. PCRs were performed using Platinum Pfx polymerase (Invitrogen, Carlsbad, CA) in 96-well plates using a 100-μL reaction mix containing 1× enhancer; 0.15 mM dATP, dGTP, dCTP, and dCTP; 1 mM $MgSO_4$; 1 μM primer; and 2 units of Platinum Pfx polymerase in 1× reaction buffer. After each amplification, 5 μL of PCR products was run in 1.2% (w/v) agarose gel to assess the quality of desired products. After successful amplification of all 3,165 genes, each plate of PCR products was purified using Multiscreen-PCR plates (Millipore, Bedford, MA) following the manufacturer's instructions. The DNA was eluted in 50 μL of water and transferred into UV-transparent 384-well plates (Corning Incorporated, Corning, NY). The yield of each purified product was measured with a Spectramax 384 plus spectrophotometer (Molecular Devices Corporation, Sunnyvale, CA). These products were then dried in a Speed Vac (Savant Instruments, Holbrook, NY). Using a Bio-robot 3000 (Qiagen, Valencia, CA), we first resuspended each product in water to give a concentration of 1 μg μL^{-1}, and then an equal volume of 2× microspotting solution (Telechem International, Sunnyvale, CA) was added. Ten microliters of each product was transferred to printing source plates (384-well plates, Genetix Limited, XXXX, UK). PCR products were printed on superamine slides (Telechem International) with 16-microquill 2000 pins (Majer Precision, Tempe, AZ) using an Omnigrid arrayer (Gene Machines, San Carlos, CA). All PCR products were printed in triplicate on each slide. Many authors have commented on the importance of sufficient replicates in the analysis of

AQ: G

microarray data, and the technical replicates were valuable in our statistical analysis (Arfin et al., 2000; Kerr and Churchill, 2001a, 2001b; Long et al., 2001; Wolfinger et al., 2001; Yang and Speed, 2002). The diameter of each spot was about 125 μm with a spacing of 250 μm between center to center of any given two spots. After printing was completed, slides were baked at 80°C for 2 h and stored in the dark at room temperature.

RNA Isolation and RNA Gel-Blot Analysis

Total RNA from *Synechocystis* sp. strain PCC 6803 was isolated using the procedure described by Reddy et al. (1990) with modifications as in Colon-Lopez et al. (1997). RNA was isolated from cells that were harvested from cultures collected after LoFe growth and 3, 12, and 24 h after the addition of iron to the iron-deficient cells. At each time point, cells were mixed with 1/20 volume of stop solution (200 mM Tris-HCl [pH 8.0], 20 mM EDTA, and 20 mM sodium azide), pelleted, and stored at −80°C.

Preparation of Fluorescently Labeled Probes

Fluorescently labeled cDNA probes were prepared from the total RNA by reverse transcription of total RNA in the presence of aminoallyl-dUTP followed by coupling either with Cy3 or Cy5 monofunctional dye (Amersham Pharmacia Biotech, Piscataway, NJ). The importance of random hexamer priming for bacterial RNA was discussed by Arfin et al. (2000), and we have optimized the priming of total RNA by using a mixture of hexamers, octamers, nanomers, and decamers. The reverse transcription reaction was performed in a 50-μL volume containing 10 μg of total RNA; 5 μg of random primers mix (containing 6:2:1:1 [w/v] hexamer:octamer:nanomer:decamer); 10 mM dithiothreitol; 0.5 mM each of dATP, dCTP, and dGTP; 0.3 mM dTTP; 0.2 mM aadUTP; and 400 units of SuperscriptII reverse transcriptase (Invitrogen) in 1× reaction buffer. RNA and primers were heated at 65°C for 5 min and chilled on ice before the remaining reaction components were added. The reverse transcription was performed for 2 h at 44°C. After reverse transcription, the RNA was degraded by incubating at 65°C for 15 min after the addition of 17 μL of 0.5 M EDTA (pH 8.0) and 17 μL of 1 N NaOH. The reaction was neutralized by the addition of 34 μL of 1 M Tris (pH 7.5). Four hundred microliters of water was added to the neutralized samples, and the mix was placed in a Microcon YM-10 microconcentrator (Millipore) and spun for 30 min in a bench-top microcentrifuge at 11,000*g*. The cDNA retained by the Microcon was washed twice with 400 μL of water after centrifugation at 11,000*g*. After the last wash, 50 μL of water was added in Microcon tubes, mixed properly by pipetting, and cDNA was transferred in a new tube. To maximize the recovery of cDNA, a second washing with 50 μL of water was also carried out. Both the eluates were combined and dried in Speed Vac. The aminoallyl labeled cDNAs were resuspended in 10 μL of water and then 10 μL of 0.2 M $NaHCO_3$ (pH 9.0) was added. This sample was transferred in a tube containing either Cy3 or Cy5 monofunctional dye and incubated for 1 h at room temperature in the dark. The uncoupled dyes were quenched by the addition of 4.5 μL of 4 M hydroxylamine after incubation for 15 min at room temperature in the dark. The unincorporated dyes from Cy3 and Cy5 reactions were separately removed using a Qia-Quick PCR purification column according to the manufacturer's instructions (Qiagen). The column eluates were combined, dried in a Speed Vac and resuspended in 40 μL of TE (10 mM Tris [pH 8.0] and 1 mM EDTA).

Hybridization, Washing, and Scanning

Before hybridization, the slides were washed once in 0.2% (w/v) SDS and twice in water for 5 min each at room temperature. Thereafter, slides were transferred in hot water for 5 min and washed in 0.2% (w/v) SDS, followed by two washes in water for 5 min each. The slides were spun dried and prehybridized in a mixture of 25% (w/v) formamide, 5× SSC, 0.1% (w/v) SDS, and 1% (w/v) bovine serum albumin for 45 min at 42°C in a CLONTECH hybridization chamber (CLONTECH, Palo Alto, CA). The slide was briefly rinsed with water and spun dried. Hybridization was carried in a total volume of 80 μL consisting of 25% (w/v) formamide, 5× SSC, 0.1% (w/v) SDS, 1% (w/v) bovine serum albumin, 0.1 mg of salmon sperm DNA, and Cy3- and Cy5-labled probes. The labeled cDNA in hybridization buffer was heated at 95°C for 2 min and quickly transferred to an oven maintained at 42°C. The slide was placed in a CMT hybridization chamber (Corning) and transferred to the oven at 42°C. After 10 min of incubation, hybridization solution containing labeled probes was placed on the slide and covered by a coverslip. The whole assembly was placed in a water bath maintained at 42°C. After 18 to 20 h of hybridization, slides were washed in 2× SSC and 0.1% (w/v) SDS, which was preheated at 42°C. After 5 min of incubation, the slides were further washed in 0.1× SSC and 0.1% (w/v) SDS for 10 min at room temperature. Finally, slides were rinsed in 0.1× SSC and then briefly in water. The slides were spun dried and immediately scanned. The scanning was performed with a Scanarray 4000 scanner (Packard BioChip Technologies, Billerica, MA) for Cy3 (532 nm) and Cy5 (635 nm) at a resolution of 10 μm per pixel generating two separate TIFF images. Images were often acquired at various laser and PMT settings.

Experimental Design

The effect of iron deficiency on gene expression in *Synechocystis* sp. PCC 6803 was studied with cultures grown in iron-deficient medium for 10 generations (0 h). Iron was then added back to the normal levels found in the BG-11 medium, and RNA was isolated at three subsequent time points (3, 12, and 24 h) because these were times of important physiological events (Riethman et al., 1988). We used a loop design that included a "dye swap" such that RNA from each time point was labeled with both Cy3 and Cy5 and was used for hybridization (Fig. 1A; Kerr and Churchill, 2001a, 2001b; Churchill, 2002; Oleksiak et al., 2002; Yang and Speed, 2002). Most importantly, this design ensures that the iron effect is not completely confounded with other potential sources of variation. It should be noted that the three replicate slides for each time point and the three replicate printings per slide represent technical variation. Biological variation was sampled by extracting RNA from three separate experiments and pooling them before all of the hybridizations.

Data Acquisition and Statistical Analysis

Spot intensities of the images were quantified using Quantarray 3.0 (Packard BioChip Technologies). A predefined grid containing a defined circle fitting the size of spots was placed on each image and manually adjusted to ensure optimal spot recognition. Spots were individually quantified using the adaptive method, and the mean intensities corresponding to each spot were exported into a separate Excel spreadsheet for each array. Data for the six slides in this experiment were then uploaded into SAS. Testing has demonstrated that Quantarray is very reliable and similar to results from Imagene 6.0 (Moody et al., 2002).

An ANOVA modeling approach was used to analyze the microarray data (Kerr and Churchill, 2001a, 2001b; Wolfinger et al., 2001; Churchill, 2002; Oleksiak et al., 2002; Wayne and McIntyre, 2002; Drenth et al., 2003). The model $Y_{ijklm} = \mu + t_i + d_j + \omega_k + \omega_k(\rho_l) + \epsilon_{ijklm}$ was fit, where Y is the intensity of the spot after correction for the local background signal, normalization, and log transformation. The parameter μ was the overall mean of the normalized values for that gene. Fixed effects for time (t) and dye (d) were fit, but the interaction was omitted because it was confounded with the effect of slide. The random effects of slide (ω) and of replicates within slide [$\omega_k(\rho_l)$] were included. To test the null hypothesis that a particular gene's expression level was not different over time, an F test of the effect of time for each gene was conducted, and a P value was calculated. We examined the model for conformation to the assumption of normality of the residuals by testing the null hypothesis that the residuals for each gene were normally distributed using the Shapiro-Wilkes Test. Additional contrasts were examined. The effect at time 0 (the iron-deficient state) was compared separately with 24 h after iron addition, time 0 was compared with time 3, time 3 was compared with time 12, and time 12 was compared with time 24. All analyses were performed in SAS (SAS Institute, 2002).

We used a Bonferroni significance level of 0.05/3,165 or 0.000015797788 as a criterion for rejecting the null hypothesis of a significant time effect. Because type I and type II errors are inversely related, with decreases in false positives (type I) being associated with increases in false negatives (type II), and because the Bonferroni correction will be overly conservative as tests are correlated (Westfall and Young, 1993; Doerge and Churchill, 1996; McIntyre et al., 2000), we used a second overly liberal threshold of 0.05. In addition, we considered the test for dye effects and normality of the residuals. If the test of the null hypothesis of difference across times was rejected at 0.0000158 and we had no evidence for dye effects or departure from normality of the residuals, we declared the gene differentially ex-

pressed over time and concluded that the changes in gene expression were statistically significant (these 85 genes are highlighted in red in Supplemental Data Table I, http://www.plantphysiol.org). If the *P* value for the test of differences over time was less than or equal to 0.05 but larger than 0.0000158 and we had no evidence for dye effects or departure from normality of the residuals, we considered the gene interesting (these 781 genes are highlighted in yellow in Supplemental Data Table I, http://www.plantphysiol.org). When dye effects were present or residuals showed evidence of departure from normality, we advise caution in the interpretation of the results. Genes that show a *P* value for the test of differential expression that exceeds the Bonferroni criteria or the liberal threshold but that have significant dye effects are indicated as dye-red or dye-yellow (Supplemental Data Table I, http://www.plantphysiol.org); genes that depart from normality are highlighted in green (Bonferroni) or blue (0.05; Supplemental Data Table I, http://www.plantphysiol.org). Once the analysis was completed, we examined the results carefully, and we focused our discussion on statistically significant and interesting genes that exhibited a fold change of at least 1.25×. This included the 85 statistically significant and 731 statistically interesting genes. A total of 10 genes with possible dye effects were included in the functional analysis (six significant and four interesting) based on independent northern-blot confirmation or cluster analysis where other genes in a transcriptional cluster were found to be significant or interesting. Genes that departed from normality of the residuals, but showed some evidence of differential expression, were individually analyzed, and 40 were included in the functional analysis. In all of these cases, the departure from normality was due to extreme differences in the response in the iron-deficient state (time 0) compared with the other three time points and the resulting heteroscedasticity of the error. There were a total of 866 genes examined with a $P < 0.05$. Our objective is to identify genes that demonstrate differential expression for further experimentation. Thus, we bracket our interpretation of the results with a conservative (Bonferroni) threshold and a liberal 0.05 criterion. The raw *P* values are available for inspection by other investigators in Supplemental Data Table I (http://www.plantphysiol.org) so that individuals may examine the evidence themselves.

Independent Validation of Microarray Results with Northern Blots

Microarray experiments provide information on the expression profiling of thousands of genes, and it is critical to have an independent measure for at least a subset of the results. Several factors such as contamination with other genes, dust or scratches on the cDNA spots, and high background can lead to false profiling. In the present study, we have utilized technical replicates on each array, multiple arrays, and a statistical analysis to identify potential problems, and then used northern blots to validate the results. In one experiment, we selected nine genes at random from among the unknown category plus a gene (sll0249) in the *isiA* region to compare expression patterns as obtained from northern blots versus those from the microarray. In general, there was an excellent qualitative correspondence between the two techniques, although there were some quantitative differences (data not shown).

Distribution of Materials

Upon request, all novel material described in this publication will be made available in a timely manner for noncommercial research purposes, subject to the requisite permission from any third party owners of all or parts of the material. Obtaining any permission will be the responsibility of the requestor.

ACKNOWLEDGMENTS

We would like to thank Hong Li for many discussions during the course of this work and Elsie Grace for her efforts on the data management. We would also like to thank Dr. Rob Burnap and his lab (especially Brad Postier) for the very fruitful collaboration that led to the construction of this microarray.

Received March 21, 2003; returned for revision April 21, 2003; accepted May 12, 2003.

LITERATURE CITED

Arfin SM, Long AD, Ito ET, Tolleri L, Riehle MM, Paegle ES, Hatfield GW (2000) Global gene expression profiling in *Escherichia coli* K12. J Biol Chem **275:** 29672–29684

Bailey S, Thompson E, Nixon PJ, Horton P, Mullineaux CW, Robinson C, Mann NH (2002) A critical role for the Var2 FtsH homologue of *Arabidopsis thaliana* in the photosystem II repair cycle *in vivo*. J Biol Chem **277:** 2006–2011

Behrenfeld MJ, Kolber ZS (1999) Widespread iron limitation of phytoplankton in the south pacific ocean. Science **283:** 840–843

Bibby TS, Nield J, Barber J (2001) Iron deficiency induces the formation of an antenna ring around trimeric photosystem I in cyanobacteria. Nature **412:** 743–745

Boekema EJ, Hlfney A, Yakushevska AE, Plotrowski M, Keegstra K, Berry S, Michel K-P, Pistorius EK, Krulp J (2001) A giant chlorophyll-protein complex induced by iron deficiency in cyanobacteria. Nature **412:** 745–748

Burnap RL, Troyan T, Sherman LA (1993) The highly abundant chlorophyll-protein complex of iron-deficient *Synechococcus* sp PCC7942 (CP43′) is encoded by the *isiA* gene. Plant Physiol **103:** 893–902

Churchill GA (2002) Fundamentals of experimental design for cDNA microarrays. Nat Genet **32:** 490–495

Colon-Lopez MS, Sherman DM, Sherman LA (1997) Transcriptional and translational regulation of nitrogenase in light-dark- and continuous-light-grown cultures of the unicellular cyanobacterium *Cyanothece* sp strain ATCC 51142. J Bacteriol **179:** 4319–4327

Doerge RW, Churchill GA (1996) Permutation tests for multiple loci affecting a quantitative character. Genetics **142:** 285–294

Drenth JPH, te Morische RHM, Smink R, Bonifacino JS, Jansen JBMJ (2003) Germline mutations in *PRKCSH* are associated with autosomal dominant polycystic liver disease. Nat Genet **33:** 1–3

Earhart C (1996) Uptake and metabolism of iron and molybdenum. *In* FC Neidhardt, ed *Escherichia coli* and *Salmonella*. ASM Press, Washington, DC, pp 1075–1090

Fox TC, Guerinot ML (1998) Molecular biology of cation transport in plants. Annu Rev Plant Physiol Plant Mol Biol **49:** 669–696

Fromme P, Jordan P, Kraus N (2001) Structure of PSI. Biochim Biophys Acta **1507:** 5–31

Garcia-Dominguez M, Muro-Pastor MI, Reyes JC, Florencio FJ (2000) Light-dependent regulation of cyanobacterial phytochrome expression. J Bacteriol **182:** 38–44

Gill R, Katsoulakis E, Schmitt W, Taroncher-Oldenburg G, Misra J, Stephanopoulos G (2002) Genome-wide dynamic transcriptional profiling of the light-to-dark transition in *Synechocystis* sp strain PCC 6803. J Bacteriol **184:** 3671–3681

Guikema JA, Sherman LA (1983) Organization and function of chlorophyll in membranes of cyanobacteria during iron starvation. Plant Physiol **73:** 250–256

Guikema JA, Sherman LA (1984) Influence of iron deprivation on the membrane composition of *Anacystis nidulans*. Plant Physiol **74:** 90–95

Hantke K (2001) Iron and metal regulation in bacteria. Curr Opin Microbiol **4:** 172–177

Hauβühl K, Andersson B, Adamska I (2001) A chloroplast DegP2 protease performs the primary cleavage of the photodamaged D1 protein in plant photosystem II. EMBO J **20:** 713–722

Heathcote P, Fyfe PK, Jones MR (2002) Reaction centers: the structure and evolution of biological solar power. Trends Biochem Sci **27:** 79–87

Hihara Y, Kamei A, Kanehisa M, Kaplan A, Ikeuchi M (2001) DNA microarray analysis of cyanobacterial gene expression during acclimation to high light. Plant Cell **13:** 793–806

Jin W, Riley RM, Wolfinger RD, White KP, Passador-Gurgel G, Gibson G (2001) The contributions of sex, genotype and age to transcriptional variance in *Drosophila melanogaster*. Nat Genet **29:** 389–395

Kaneko T, Sato S, Kotani H, Tanaka A, Asamizu E, Nakmura Y, Miyajima N, Hirosawa M, Sugiura M, Sasamoto S et al. (1996) Sequence analysis of the genome of the unicellular cyanobacterium *Synechocystis* sp strain 6803: II. Sequence determination of the entire genome and assignment of potential protein-coding regions. DNA Res **3:** 109–136

Kanesaki Y, Suzuki I, Allakhverdiev SI, Mikami K, Murata N (2002) Salt stress and hyperosmotic stress regulate the expression of different sets of genes in *Synechocystis* sp PCC 6803. Biochem Biophys Res Commun **290:** 339–344

Katoh H, Hagino N, Grossman AR, Ogawa T (2001) Genes essential to iron transport in the cyanobacterium *Synechocystis* sp strain PCC 6803. J Bacteriol **183:** 2779–21784

Katoh H, Grossman AR, Hagino N, Ogawa T (2000) A gene of *Synechocystis* sp strain PCC 6803 encoding a novel iron transporter. J Bacteriol **182:** 6523–6524

Kerr MK, Churchill GA (2001a) Statistical design and the analysis of gene expression microarrays. Genet Res **77:** 123–128

Kerr MK, Churchill GA (2001b) Experimental design for gene expression microarrays. Biostatistics **2:** 183–201

Komenda J, Lupinkova L, Kopecky J (2002) Absence of the *psbH* gene product destabilizes photosystem II complex and bicarbonate binding on its acceptor side in *Synechocystis* sp PCC 6803. Eur J Biochem **269:** 610–619

Lamparter T, Esteban B, Hughes J (2001) Phytochrome Cph1 from the cyanobacterium *Synechocystis* PCC6803. Eur J Biochem **268:** 4720–4730

Laudenbach DE, Reith ME, Straus NA (1988) Isolation, sequence analysis, and transcriptional studies of the flavodoxin gene from *Anacystis nidulans* R2. J Bacteriol **170:** 258–265

Laudenbach DE, Straus NA (1988) Characterization of a cyanobacterial iron stress-induced gene similar to psbC J. Bacteriol **170:** 5018–5026

Lindahl M, Spetea C, Hundal T, Oppenheim AB, Adam Z, Andersson B (2000) The thylakoid FtsH protease plays a role in the light-induced turnover of the photosystem II D1 protein. Plant Cell **12:** 419–431

Long AD, Mangalam HJ, Chan BYP, Tolleri L, Hatfield GW, Baldi P (2001) Improved statistical inference from DNA microarray data using analysis of variance and a bayesian statistical framework. J Biol Chem **276:** 19937–19944

Mann NH, Novac N, Mullineaux CW, Newman J, Bailey S, Robinson C (2000) Involvement of an FtsH homologoue in the assembly of functional photosystem I in the cyanobacterium *Synechocystis* sp PCC 6803. FEBS Lett **479:** 72–77

McIntyre L, Martin E, Simonsen K, Kaplan N (2000) Circumventing multiple testing: a multilocus Monte Carlo approach to testing for association. Genet Epidemiol **19:** 18–29

Michel KP, Krüger F, Pühler A, Pistorius EK (1999) Molecular characterization of *idiA* and adjacent genes in the cyanobacteria *Synechococcus* sp strains PCC 6301 and PCC 7942. Microbiology **145:** 1473–1484

Michel K-P, Pistorius EK, Golden SS (2001) Unusual regulatory elements for iron deficiency induction of the *idiA* gene of *Synechococcus elongatus* PCC 7942. J Bacteriol **183:** 5015–5024

Michel K-P, Thole HH, Pistorius EK (1996) IdiA, a 34 kDa protein in the cyanobacteria *Synechococcus* sp strains PCC 6301 and PCC 7942, is required for growth under iron and manganese limitations. Microbiology **142:** 2635–2645

AQ: Q **Moody D, Fadlia B, Singh A, Shah S, McIntyre LM** (2002) Quantitative comparison of image analysis software. DNA Press (in press)

Negishi T, Nakanishi H, Yazaki J, Koshimoto N, Fujii F, Shimbo K, Yamamoto K, Sakata K, Sasaki T, Kikuchi S et al. (2002) cDNA microarray analysis of gene expression during Fe-deficiency stress in barley suggests that polar transport of vesicles is implicated in phytosiderophore secretion in Fe-deficient barley roots. Plant J **30:** 83–94

Oleksiak MF, Churchill GA, Crawford DL (2002) Variation in gene expression within and among natural populations. Nat Genet **32:** 261–266

Pakrasi HB, Goldenberg A, Sherman LA (1985a) Membrane development in the cyanobacterium, *Anacystis nidulans*, during recovery from iron starvation. Plant Physiol **79:** 290–295

Pakrasi HB, Riethman HC, Sherman LA (1985b) Organization of pigment proteins in the photosystem II complex of the cyanobacterium *Anacystis* AQ: R *nidulans* R2. Proc Natl Acad Sci USA **82:** 6903–6907

Park C-M, Kim J-I, Yang S-S, Kang J-G, Kang J-H, Shim J-Y, Chung Y-H, Park Y-M, Song P-S (2000a) A second photochromic bacteriophytochrome from *Synechocystis* sp PCC 6803: spectral analysis and down-regulation by light. Biochem **39:** 10840–10847

Park C-M, Shim J-Y, Yang S-S, Kang J-G, Kim J-I, Luka Z, Song P-S (2000b) Chromophore-apoprotein interactions in *Synechocystis* sp PCC6803 phytochrome Cph1. Biochemistry **39:** 6349–6356

Paustian M, May BJ, Kapur V (2001) *Pasteurella multocida* gene expression in response to iron limitation. Infect Immun **69:** 4109–4115

Pérez-Amador M, Lidder P, Johnson MA, Landgraf J, Wisman E, Green PJ (2001) New molecular phenotypes in the *dst* mutants of *Arabidopsis* Revealed by DNA microarray analysis. Plant Cell **13:** 2703–2717

Ratledge C, Dover LG (2000) Iron metabolism in pathogenic bacteria. Annu Rev Microbiol **54:** 881–9941

Reddy KJ, Webb R, Sherman LA (1990) Bacterial RNA isolation with one hour centrifugation in a table-top ultracentrifuge. BioTechniques **8:** 250–251

Richmond CS, Glasner JD, Mau R, Jin H, Blattner FR (1999) Genome-wide expression profiling in *Escherichia coli* K-12. Nucleic Acids Res **27:** 3821–3835

Riethman HC, Bullerjahn G, Reddy KJ, Sherman LA (1988) Regulation of cyanobacterial pigment-protein composition and organization by environmental factors. Photosynth Res **18:** 133–161

Seki M, Narusaka M, Abe H, Kasuga M, Yamaguchi-Shinozaki Y, Carninci P, Hayashizaki Y, Shinozaki K (2001) Monitoring the expression pattern of 1300 *Arabidopsis* genes under drought and cold stresses by using a full-length cDNA microarray. Plant Cell **13:** 61–72

Sherman DM, Sherman LA (1983) Effect of iron deficiency and iron restoration on ultrastructure of *anacystis nidulans*. J Bacteriol **156:** 393–401

Singh AK, Sherman LA (2000) Identification of iron-responsive differential gene expression in the cyanobacterium *Synechocystis* sp strain PCC 6803 with a customized amplification library. J Bacteriol **182:** 3536–3543

Singh AK, Sherman LA (2002) Characterization of a stress-responsive operon in the cyanobacterium *Synechocystis* sp strain PCC 6803. Gene **297:** 11–19

Straus NA (1994) Iron deprivation: physiology and gene regulation. *In* DA Bryant, ed, The Molecular Biology of Cyanobacteria. Kluwer Academic Publishers, Dordrecht, The Netherlands, pp 731–750

Suzuki I, Kanesaki Y, Mikami K, Kanehisa M, Murata N (2001) Cold-regulated genes under control of the cold sensor Hik33 in *Synechocystis*. Mol Microbiol **40:** 235–244

Tao H, Bausch C, Richmond C, Blattner FR, Conway T (1999) Functional genomics: expression analysis of *Escherichia coli* growing on minimal and rich media. J Bacteriol **181:** 6425–6440

Thimm O, Essigmann B, Kloska S, Altmann T, Buckhout TJ (2001) Response of *Arabidopsis* to iron deficiency stress as revealed by microarray analysis. Plant Physiol **127:** 1030–1043

Ting CS, Rocap G, King J, Chisholm SW (2002) Cyanobacterial photosynthesis in the oceans: the origins and significance of divergent light-harvesting strategies. Trends Microbiol **10:** 134–142

Tölle J, Michel K-P, Kruip J, Kahmann U, Preisfeld A, Pistorius EK (2002) Localization and function of the IdiA homologue Slr1295 in the cyanobacterium *Synechocystis* sp strain PCC 6803. Microbiology **148:** 3293–3305

Vinnemeier J, Kunert A, Hagemann M (1998) Transcriptional analysis of the *isiAB* operon in salt-stressed cells of the cyanobacterium *Synechocystis* sp PCC 6803. FEMS Microbiol Lett **169:** 323–330

Wayne ML, McIntyre LM (2002) Combining mapping and arraying: an approach to candidate gene identification. Proc Natl Acad Sci USA **99:** 14903–14906

Westfall PH, Young SS (1993) Resampling-Based Multiple Testing: Examples and Methods for P-Value. John Wiley Sons, Inc., Somerset, NJ

Wilde A, Fielder B, Börner T (2002) The cyanobacterial phytochrome Cph2 inhibits phototaxis towards blue light. Mol Microbiol **44:** 981–988

Wolfinger RD, Gibson E, Wolfinger L, Bennett H, Hamadeh P, Bushel CA, Paules RS (2001) Assessing gene significance from cDNA microarray expression data via mixed models. J Comput Biol **8:** 625–637

Xu W, Tang H, Wang Y, Chitnis PR (2001) Proteins of the cyanobcacterial photosystem I. Biochim Biophys Acta **1507:** 32–40 AQ: S

Yang IV, Chen E, Hasseman JP, Liang W, Frank BC, Wang S, Sharov V, Saeed AI, White J, Li J et al. (2002) Within the fold: assessing differential expression measures and reproducibility in microarray assays. Genome Biol **3:** xxx–xxx

Yang YH, Speed T (2002) Design issues for cDNA microarray experiments. Nat Rev Gen **3:** 579–588

Yeh K-C, Wu S-H, Murphy JT, Lagarias JC (1997) A cyanobacterial phytochrome two-component light sensory system. Science **277:** 1505–1508

Yue H, Eastman PS, Wang BB, Minor J, Doctolero MH, Nuttall RL, Stack R, Becker JW, Montgomery JR, Vainer M et al. (2001) An evaluation of the performance of cDNA microarrays for detecting changes in global mRNA expression. Nucleic Acids Res **29:** E41–1

Zouni A, Witt H-T, Kern J, Fromme P, Kraus N, Saenger W, Orth P (2001) Crystal structure of photosystem II from *Synechococcus elongatus* at 38Å resolution. Nature **409:** 739–743

AUTHOR QUERIES

AUTHOR PLEASE ANSWER ALL QUERIES 1

A—Au: Please confirm that correct italicization is used throughout the paper.

B—Au: Please provide species name for *Prochlorococcus*. Per journal style, a genus name must be accompanied by a species name.

C—Au: Changed spelling to Pérez-Amador to match reference list. Correct?

D—Au: Please confirm/correct Stillwater as location for Oklahoma State University.

E—Au: Per journal style, initial callouts of figures must appear in numerical order. Please move this citation of Figure 3 to after the Figure 2 citation in the text or renumber figures accordingly.

F—Au: Changed spelling to Garcia-Dominguez to match reference list. Correct?

G—Au: Please provide city location for Genetix Limited.

H—Au: Please confirm/correct 6:2:1:1 [w/v] hexamer:octamer:nanomer:decamer.

I—Au: Please confirm/correct dithiothreitol as expansion for DTT. Per journal style, nonstandard abbreviations must be used at least three times in the text.

J—Au: Please confirm/correct 0.2% (w/v) SDS here and in the next sentence.

K—Au: Please confirm/correct 25% (w/v) formamide.

L—Au: Please confirm/correct 0.1% (w/v) SDS here and throughout the paragraph.

M—Au: Please confirm/correct 1% (w/v) bovine serum albumin here and later in the paragraph.

N—Au: Please confirm/correct 25% (w/v) formamide.

O—Au: Please spell out PMT. Per journal style, nonstandard abbreviations must be used at least three times in the text.

P—Au: This citation (SAS Institute, 2002) was not included in the reference list. Please add corresponding reference or delete citation from the text.

Q—Au: If possible, please update Moody et al. (2002).

R—Au: Please note that Park et al. 2002a and 2002b have been switched to accommodate proper alphabetization in the reference list. Please verify that in-text citations are accurate.

AUTHOR QUERIES

AUTHOR PLEASE ANSWER ALL QUERIES **2**

S—Au: Please provide page range for Yang et al. (2002).

T—Au: Please spell out IFAFS.

U—Au: Please provide manufacturer's name and city/state/country location for Spotfire Decisionsite version 7.0.